Society of Medical Education & Research

2026, Volume 6, Issue 1, Page No: 141-153
ISSN: 3108-4834

Archive of International Journal of Cancer and Allied Science

Predictive Performance of Machine Learning-Based Classification Using Conventional 18F-FDG PET Parameters for Identifying Postsurgical Aggressive Features of Endometrial Cancer

Saif Al-Hinai[1]*, Amal Al-Balushi[1], Mohammed Al-Maskari[2], Sultan Al-Mahruqi[3]

[1]Department of Endometrial Cancer and Machine Learning, College of Medicine, Sultan Qaboos University, Muscat, Oman.
[2]Department of PET Parameters and Aggressive Features, College of Medicine, University of Nizwa, Nizwa, Oman.
[3]Department of Postsurgical Prediction and AI, College of Medicine, Dhofar University, Salalah, Oman.

***E-mail** ✉ saif.alhinai@squ.edu.om

Abstract

To evaluate the preoperative value of ML-driven classification based on conventional 18F-FDG PET metrics and clinical information for forecasting features of EC aggressiveness. A retrospective analysis was conducted on 123 patients with EC who received 18F-FDG PET scans for preoperative staging between 2009 and 2021. SUVmax, SUVmean, metabolic tumor volume (MTV), and total lesion glycolysis (TLG) were measured from the primary lesion. Patient age and body mass index (BMI) were recorded. Histological subtype, depth of myometrial invasion (MI), risk category, lymph node (LN) status, and p53 expression were obtained from pathology reports. The cohort was randomly partitioned into training (80%) and validation (20%) subsets. The training data served for feature selection (via Mann-Whitney U test and ROC analysis) and model development, while the validation set assessed predictive performance. In the validation cohort, the highest accuracies achieved were: 61% using TLG alone versus 87% with ML for deep MI; 71% using SUVmax alone versus 79% with ML for risk group classification; 72% using TLG alone versus 83% with ML for LN involvement; and 45% using SUVmax or SUVmean alone versus 73% with ML for p53 expression. Classification models based on ML integrating standard 18F-FDG PET parameters and clinical data effectively characterized the examined features of EC aggressiveness. This offers a non-invasive approach to aid preoperative risk stratification in EC patients.

Keywords: Endometrial cancer, 18F-FDG PET, Machine learning, Prognostic value, Imaging parameters

Introduction

Endometrial cancer (EC) represents the leading gynecologic malignancy in high- and middle-income nations [1]. Its incidence increases with factors such as obesity, advanced age, early onset of menstruation, and delayed menopause [2, 3]. Histologically, EC is divided into endometrioid carcinomas, which comprise 70–80% of cases [4], and non-endometrioid types (10–20%), including serous, clear-cell, mixed, and other uncommon variants, which are associated with poorer outcomes [5]. Optimal therapeutic strategies require timely and reliable determination of disease status and biological aggressiveness. Management options encompass surgical procedures, radiotherapy, conventional chemotherapy, and endocrine therapy [1]. Additionally, immune checkpoint inhibitors and VEGF-targeted agents have demonstrated promising effectiveness and tolerability in advanced endometrial carcinoma [6].

Extensive surgery combined with lymph node dissection is typically advised for individuals at elevated risk. Nevertheless, accurately identifying suitable candidates for such interventions remains difficult [7]. This is

Access this article online https://smerpub.com/

Received: 21 January 2026; **Accepted:** 27 April 2026

How to cite this article: Al-Hinai S, Al-Balush A, Al-Maskari M, Al-Mahruqi S. Predictive Performance of Machine Learning-Based Classification Using Conventional 18F-FDG PET Parameters for Identifying Postsurgical Aggressive Features of Endometrial Cancer. Arch Int J Cancer Allied Sci. 2026;6(1):141-53. https://doi.org/10.51847/HVcF6AtLzy

particularly relevant for younger women who may wish to preserve fertility, where conservative management options must be weighed [8-10]. Key indicators of EC aggressiveness include FIGO stage, histologic type, extent of myometrial invasion (MI) [7], and lymph node (LN) metastasis [11-13]. Furthermore, molecular profiling has gained prominence in risk assessment, as genomic characteristics significantly affect disease progression and survival [14, 15]. Overexpression of p53, in particular, serves as an important prognostic marker in EC and interacts with various genetic elements, including PTEN, which is linked to adverse outcomes across multiple malignancies [5, 16-18].

A major constraint is that most of these aggressiveness features become available only postoperatively, with limited options for preoperative evaluation even on biopsy specimens. Biopsies may fail to capture intratumoral heterogeneity, thus offering incomplete insights into tumor behavior before surgery [19, 20]. Alternative methods, such as genomic and proteomic profiling, have advanced personalized care by revealing molecular pathways that influence treatment response [21].

Standard imaging techniques such as transvaginal ultrasound, MRI, and CT primarily provide anatomic details with limited functional insights [22, 23]. In contrast, 18F-FDG PET/CT plays a recognized role in preoperative EC staging and is recommended in clinical guidelines [24, 25]. It enables comprehensive whole-body evaluation, facilitating detection of nodal disease and distant spread [26-30].

While medical images are routinely interpreted qualitatively by specialists, there is growing emphasis on extracting quantitative imaging biomarkers [31] to better assess tumor biology and heterogeneity [32]. In 18F-FDG PET, commonly studied metrics include SUVmax, SUVmean, MTV, and TLG. These are established as indicators of underlying pathophysiological activity in various cancers [33-36]. Unlike more complex radiomic signatures still under exploration, these conventional parameters offer strong clinical feasibility and interpretability: they can be readily calculated using routine software during standard image review and directly relate to known biological tumor processes. These attributes address key barriers to the translation of advanced radiomics into everyday practice.

Concurrently, machine learning (ML) has emerged as a valuable tool in healthcare research to assist clinical decisions [37]. By analyzing historical patient data, ML algorithms can forecast outcomes—such as aggressiveness traits that are typically confirmed only after surgery—thereby facilitating improved risk stratification and individualized treatment.

The current investigation examines the capacity of ML models to predict multiple features of EC aggressiveness before surgery. Conventional 18F-FDG PET parameters (SUVmax, SUVmean, MTV, and TLG) were analyzed both independently and in combination with routine clinical information within ML frameworks. The goal was to enhance EC patient stratification and management in a manner that is both clinically meaningful and readily implementable.

Materials and Methods

Patients

This retrospective single-center study enrolled all consecutive patients with histologically confirmed EC who underwent 18F-FDG PET/CT at the Nuclear Medicine Unit of IRCCS San Raffaele Scientific Institute between August 2009 and February 2021 for initial staging. Eligibility required (i) a confirmed histologic diagnosis of EC and (ii) availability of a staging 18F-FDG PET scan. Cases lacking sufficient imaging, clinical, or pathologic data were excluded.

Collected variables included age, BMI, histologic subtype (endometrioid versus non-endometrioid), deep myometrial invasion (defined as >50% MI), EC risk category, LN involvement, and p53 status (mutant-type overexpression versus wild-type). Risk groups were classified as low risk (low and intermediate) or high risk (high-intermediate and high) per the ESMO-ESGO-ESTRO guidelines [24].

Separate subcohorts were formed based on the availability of specific histologic information, given the multiple predictive endpoints examined. The study received approval from the Institutional Ethics Committee of IRCCS San Raffaele Scientific Institute (138/INT/2021). All participants provided informed consent, and the protocol adhered to the Declaration of Helsinki (1964) and subsequent revisions.

18F-FDG PET protocols

Patient preparation, tracer administration, and scanning procedures followed previously reported standards [22]. Due to the retrospective nature of the study, imaging was performed on multiple systems: (1) SIGNA PET/MRI (3T, GE Healthcare), (2) Discovery ST (GE), (3)

Discovery STE (GE), (4) Gemini GXL (Philips), and (5) Discovery 690 (GE). Acquisition modes varied: 2-D (4 min/bed) on Discovery ST; 3-D on the remaining systems with bed times of 4 min (PET/MRI), 2.5 min (Discovery STE), 3 min (Discovery 690), and 2 min (Gemini GXL). Raw PET data underwent standard corrections for random coincidences, scatter, and attenuation before reconstruction. To mitigate variability arising from differences in scanners and reconstruction protocols, the ComBat harmonization technique [38] was applied to the imaging parameters.

18F-FDG PET qualitative and semiquantitative image analysis

Image interpretation was performed by two seasoned nuclear medicine specialists using the Advanced Workstation (AW; General Electric Healthcare, Waukesha, WI, USA). This platform enabled multiplanar visualization of the PET data in axial, coronal, and sagittal orientations. The scans underwent qualitative assessment, with the two readers reaching agreement on every case included in the investigation. Areas of 18F-FDG accumulation were deemed abnormal if they exceeded background physiological uptake. When abnormal uptake was identified, its precise anatomical site was determined using corresponding morphological imaging.

For the semiquantitative evaluation, volumes of interest (VOIs) were delineated semi-automatically around regions of pathological tracer accumulation within the primary tumor on transaxial slices. The following three-dimensional PET parameters were then quantified: (1) SUVmax, (2) SUVmean, (3) MTV, and (4) TLG. In the few scans lacking detectable pathological 18F-FDG uptake at the primary tumor site, a default value of 0.1 was assigned to all parameters.

Surgery and histopathological analysis

Surgical treatment was performed in 120 of 123 patients within 1 month of the 18F-FDG PET examination. Procedures typically involved total hysterectomy (via open or laparoscopic approach), bilateral salpingo-oophorectomy, peritoneal lavage, and nodal assessment through pelvic and/or para-aortic lymphadenectomy or sentinel lymph node (SLN) biopsy. A gynecologic oncology pathologist with over 30 years of experience, unaware of the PET results, conducted a detailed histologic review of all specimens, examining multiple sections per case. Data recorded included histologic subtype, pattern of myometrial infiltration, and lymph node status. Additionally, p53 immunohistochemistry results were evaluated and categorized as mutant (overexpressed) or wild-type (null).

Histopathologic findings from lymphadenectomy, SLN dissection, or subsequent imaging follow-up served as the reference standard for nodal staging. Disease stage was assigned according to the FIGO system for endometrial tumors. The three patients who did not undergo surgery were included only in evaluations of EC risk group and histologic subtype, with biopsy results used as the reference.

Statistical analysis

Statistical evaluations were conducted to determine the ability of 18F-FDG PET metrics, together with established preoperative clinical variables such as age and BMI, to predict various aspects of tumor aggressiveness. These included histologic subtype (endometrioid versus non-endometrioid), deep myometrial invasion, EC risk category (low/intermediate versus high-intermediate/high risk), lymph node involvement, and p53 marker status (overexpressed versus null).

The Kolmogorov-Smirnov test was used to assess the normality of parameter distributions. For each aggressiveness feature, the relevant patient cohort was randomly divided into a training set (80%) and a validation set (20%) using stratified sampling without overlap. On the training data, the Mann-Whitney U test was applied. To control for multiple comparisons and reduce false positives, the Benjamini-Hochberg procedure was used to adjust p-values. Parameters with adjusted p-values below 0.05 were retained for further evaluation.

Receiver operating characteristic (ROC) curve analysis assessed the discriminatory performance of individual PET and clinical variables. The area under the curve (AUC) with 95% confidence intervals (CI) enabled performance comparison, and optimal cut-off thresholds were identified using the Youden Index (the point closest to the upper-left corner of the ROC plot). These cut-offs were then applied to classify patients in the independent validation set. Predictions were compared against reference standards via confusion matrices, from which accuracy, sensitivity, specificity, negative predictive value (NPV), and positive predictive value (PPV) were calculated and contrasted. All statistical computations were executed in Python 3.7 (Scotts Valley, CA, USA).

Machine learning

Dedicated machine learning models were developed and fine-tuned for the prediction of each EC aggressiveness feature: deep myometrial invasion, risk group classification, lymph node involvement, and p53 expression status.

A Random Forest Classifier (RFC) was selected as the base algorithm for all endpoints. RFCs utilize bootstrap sampling and random feature selection at each split, making them robust to multicollinearity issues by naturally reducing the influence of redundant variables. This property is especially advantageous when incorporating conventional PET parameters, which frequently exhibit high inter-correlation.

For every model, the following workflow was followed. To prevent data leakage, input feature selection relied exclusively on the training set. Only variables previously shown to have prognostic relevance (as detailed in Section 2.5) were considered, excluding those whose 95% CI for AUC included no discriminative value. Hyperparameter optimization was likewise confined to the training data. The finalized models were then evaluated on the held-out validation set, with performance quantified through accuracy, sensitivity, specificity, NPV, and PPV. Model development and testing utilized the Scikit-learn library [39] in Python 3.7 (Scotts Valley, CA, USA).

Results and Discussion

Patients' population

The study population comprised 123 patients with biopsy-confirmed EC who underwent 18F-FDG PET for staging. Of these, 38/123 received PET/MRI, and 85/123 underwent PET/CT. To minimize variability due to differences in scanner hardware and reconstruction protocols, the ComBat harmonization approach [23] was implemented, and the adjusted PET parameters were employed in all subsequent analyses. Prior evaluations had confirmed comparable spatial resolution performance across the scanners [40-43].

Mean patient age was 65 years (standard deviation: 10.74), and mean BMI was 27 (standard deviation: 5.42). Because data availability varied across endpoints, distinct subpopulations were analyzed for each aggressiveness feature. Endometrioid histology was observed in 85 of 123 patients (69.1%). Deep myometrial invasion (>50%) was present in 53 of 115 patients (46.1%). High-intermediate or high-risk classification was applied to 76/119 patients (66.4%). p53 overexpression was noted in 37/51 patients (72.5%). Lymph node involvement analysis included 90 patients, of whom 46 underwent systematic pelvic lymphadenectomy, 23 underwent biopsy sampling, 19 underwent SLN dissection, and 2 were assessed via imaging and clinical follow-up (minimum 1 year post-surgery). Overall, nodal metastases were identified in 14 of 90 patients (15.5%).

Pathological 18F-FDG uptake corresponding to the primary tumor was visible in 119/123 cases (96.7%).

Patients' demographics and tumor characteristics are presented in **Table 1**.

Table 1. Baseline demographic and clinicopathological characteristics of the study population

Parameter	Findings
Total number of patients	123
Age, mean (SD) (years)	65 (10.74)
Body mass index (BMI). mean (SD)	27 (5.42)
FIGO stage, n (%)	
Stage I	82/123 (66.7%)
Stage II	12/123 (9.7%)
Stage III	23/123 (18.7%)
Stage IV	6/123 (4.8%)
Tumor histological classification, n (%)	
Endometrioid carcinoma	85/123 (69.0%)
Non-endometrioid carcinoma	38/123 (31.0%)
Depth of myometrial invasion, n (%)	
Less than 50% invasion	53/115 (46.1%)
50% or greater invasion	62/115 (53.9%)
Endometrial cancer risk stratification, n (%)	
Low/intermediate-risk category	43/119 (36.1%)

High-intermediate/high-risk category	76/119 (63.9%)
Lymph node (LN) involvement, n (%)	
Positive lymph node status	14/90 (15.6%)
Negative lymph node status	76/90 (84.4%)
p53 immunohistochemical status, n (%)	
p53 overexpression pattern	37/51 (72.5%)
p53 null pattern	14/51 (27.5%)
18F-FDG PET/CT findings, n (%)	
Abnormal metabolic uptake	119/123 (96.7%)
No abnormal metabolic uptake	4/123 (3.3%)

Continuous variables are reported as mean and standard deviation (SD), whereas categorical variables are presented as number/total (%) values. Abbreviations: FIGO = International Federation of Gynecology and Obstetrics; EC = endometrial cancer; LN = lymph node; SUV = standardized uptake value; MTV = metabolic tumor volume; TLG = total lesion glycolysis.

Predictive value of PET and clinical parameters

The quantitative 18F-FDG PET metrics demonstrated useful discriminatory power for distinguishing patients across most examined characteristics of EC aggressiveness, except histologic subtype **(Table 2 and Figure 1)**. Specifically, both SUVmax and SUVmean effectively separated cases based on the presence of deep myometrial invasion and risk group classification. SUVmean additionally showed value in differentiating p53 expression status. MTV and TLG further demonstrated the capacity to distinguish between groups for deep myometrial invasion, risk category, lymph node involvement, and p53 status. In contrast, the clinical variables of age and BMI showed limited predictive utility overall, with only age able to differentiate patients with deep myometrial invasion.

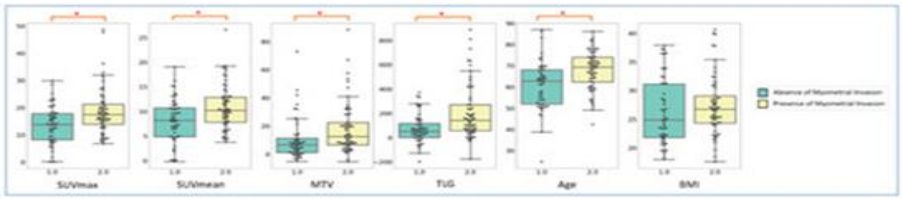

a)

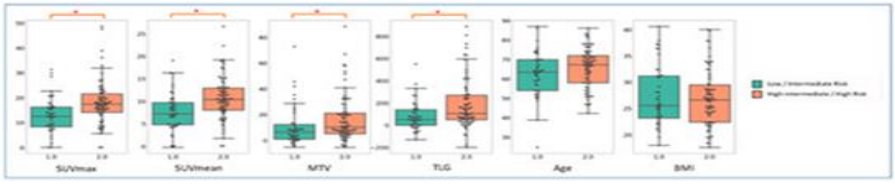

b)

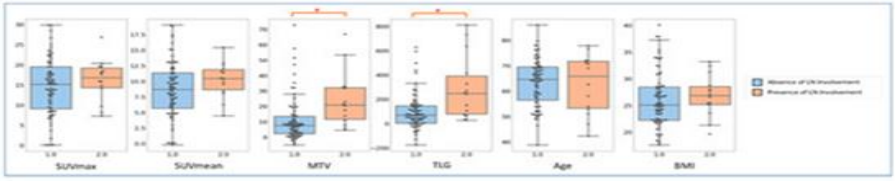

c)

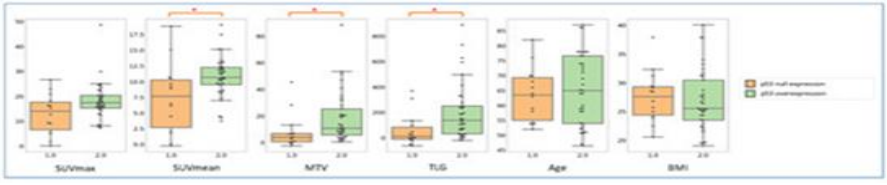

d)

Figure 1. Overview of how 18F-FDG PET metrics and clinical variables are distributed in relation to key markers of EC aggressiveness. The boxplots show the spread of each parameter for the following categories

(a) deep myometrial invasion exceeding 50%; (b) risk group stratification; (c) lymph node (LN) involvement; and (d) p53 expression status. Statistically significant differences, determined by the adjusted P-value (< 0.05) from the Mann-Whitney U test, are highlighted with red asterisks. SUV = standardized uptake value; MTV = metabolic tumor volume; TLG = total lesion glycolysis; BMI = body mass index.

Table 2. Comparison of the distribution of ^{18}F-FDG PET and clinical parameters between the groups defined by the different features of EC aggressiveness.

Feature of EC aggressiveness	SUVmean	SUVmax	TLG	MTV	BMI	Age
Histological subtype						
P-value	0.134	0.080	0.389	0.556	0.432	0.405
Adjusted P-value	0.402	0.402	0.518	0.556	0.518	0.518
Myometrial Invasion						
P-value	0.007 *	0.001 *	< 0.001 *	0.002 *	0.117	< 0.001 *
Adjusted P-value	0.008 *	0.002 *	0.001 *	0.003 *	0.117	0.001 *
EC Risk Group						
P-value	< 0.001 *	< 0.001 *	0.005 *	0.016 *	0.991	0.109
Adjusted P-value	< 0.001 *	< 0.001 *	0.010 *	0.024 *	0.991	0.131
LN Involvement						
P-value	0.126	0.341	0.003 *	0.001 *	0.316	0.929
Adjusted P-value	0.252	0.409	0.009 *	0.006 *	0.409	0.929
p53 Expression						
P-value	0.013 *	0.051	0.006 *	0.008 *	0.499	0.704
Adjusted P-value	0.026 *	0.076	0.024 *	0.024 *	0.599	0.704

The P-values obtained from the Mann–Whitney U test were corrected for multiple comparisons using the Benjamini–Hochberg false discovery rate adjustment. Abbreviations: EC = endometrial cancer; LN = lymph node. * indicates statistical significance.

The parameters SUVmax and SUVmean were found to have predictive utility for identifying deep myometrial invasion (MI) along with the EC risk category and p53 expression status. Meanwhile, MTV and TLG offered notable potential for forecasting deep MI, EC risk stratification, lymph node (LN) metastasis, and p53 expression. On the other hand, histological subtype could not be predicted by any of the evaluated metrics. Patient age and BMI generally showed weak predictive performance, except for age, which was the sole predictor of deep MI. Detailed information on AUCs, including 95% confidence intervals, optimal cut-off thresholds, sensitivity, and specificity derived from the training dataset, is provided in **Table 3**. The corresponding ROC curves are shown in **Figure 2**.

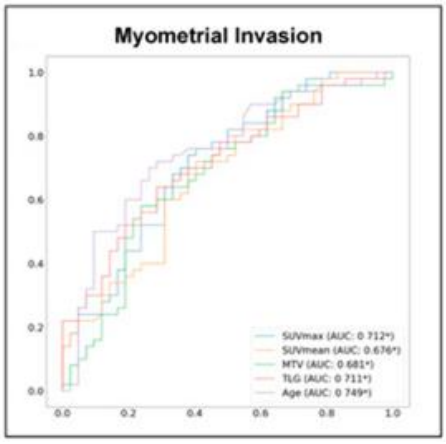

a)

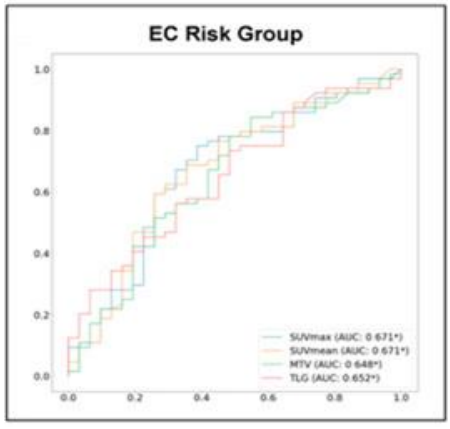

b)

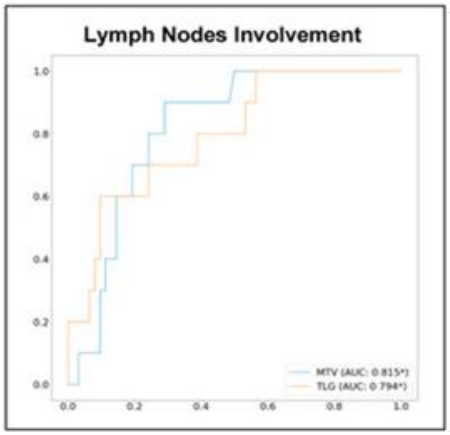

c)

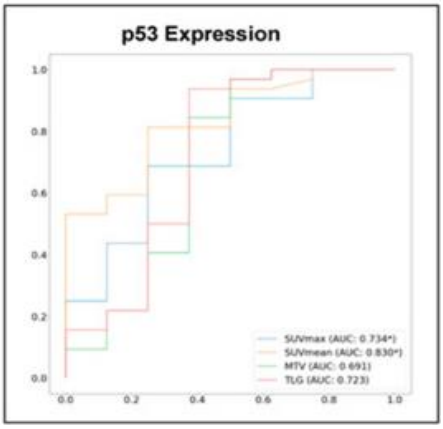

d)

Figure 2. Receiver operating characteristic curves depicting 18F-FDG PET metrics together with clinical factors for predicting multiple indicators of endometrial carcinoma (EC) aggressive behavior.

Solid lines illustrate the AUC results for SUVmax (light blue), SUVmean (orange), MTV (green), TLG (red), and patient age (purple) across the following outcomes: (a) deep myometrial invasion exceeding 50%; (b) EC risk group assignment; (c) lymph node involvement; (d) p53 expression status. Values of AUC accompanied by statistically significant 95 percent confidence intervals are denoted with an asterisk (*). Abbreviations: SUV = standardized uptake value; MTV = metabolic tumor volume; TLG = total lesion glycolysis.

Table 3. Predictive value of ^{18}F-FDG PET and clinical parameters with respect to features of EC aggressiveness on the training set.

Features of EC aggressiveness	SUVmean	SUVmax	TLG	MTV	BMI	AGE
Histological subtype						
AUC	0.458	0.421	0.469	0.473	0.566	0.418
95% CI	0.33–0.59	0.29–0.55	0.35–0.59	0.35–0.60	0.45–0.69	0.29–0.55
Optimal cut–off	/	/	/	/	/	/
Sensitivity	/	/	/	/	/	/
Specificity	/	/	/	/	/	/
Myometrial invasion						
AUC	0.676	0.712	0.711	0.681	0.564	0.749
95% CI	0.56–0.79 *	0.60–0.81 *	0.60–0.81 *	0.57–0.79 *	0.44–0.69	0.64–0.85 *
Optimal cut–off	8.556	14.850	96.125	10.980	/	66.449
Sensitivity	72%	74%	64%	58%	/	70%
Specificity	60%	62%	71%	76%	/	73%
EC risk group						
AUC	0.671	0.671	0.652	0.648	0.482	0.602
95% CI	0.55–0.79 *	0.55–0.79 *	0.53–0.77 *	0.52–0.77 *	0.35–0.61	0.48–0.72
Optimal cut–off	9.694	14.188	96.125	5.133	/	/
Sensitivity	63%	75%	56%	78%	/	/
Specificity	71%	61%	68%	52%	/	/
LN involvement						
AUC	0.611	0.577	0.794	0.815	0.579	0.523
95% CI	0.42–0.78	0.40–0.74	0.64–0.93 *	0.70–0.91 *	0.38–0.76	0.29–0.75
Optimal cut–off	/	/	251.823	10.980	/	/
Sensitivity	/	/	60%	90%	/	/
Specificity	/	/	90%	71%	/	/

p53 expression						
AUC	0.830	0.734	0.723	0.691	0.455	0.533
95% CI	0.67–0.96 *	0.52–0.93 *	0.43–0.99	0.41–0.96	0.23–0.68	0.31–0.74
Optimal cut–off	9.536	16.286	/	/	/	/
Sensitivity	81%	69%	/	/	/	/
Specificity	75%	75%	/	/	/	/

Abbreviations: AUC = area under the curve; CI = confidence interval; EC = endometrial cancer; LN = lymph node; * statistical significance. SUV = standardized uptake value; MTV = metabolic tumor volume; TLG = total lesion glycolysis; BMI = body mass index.

A representative patient case illustrating the corresponding PET parameter values and aggressive features of endometrial cancer (EC) is presented in **Figure 3**.

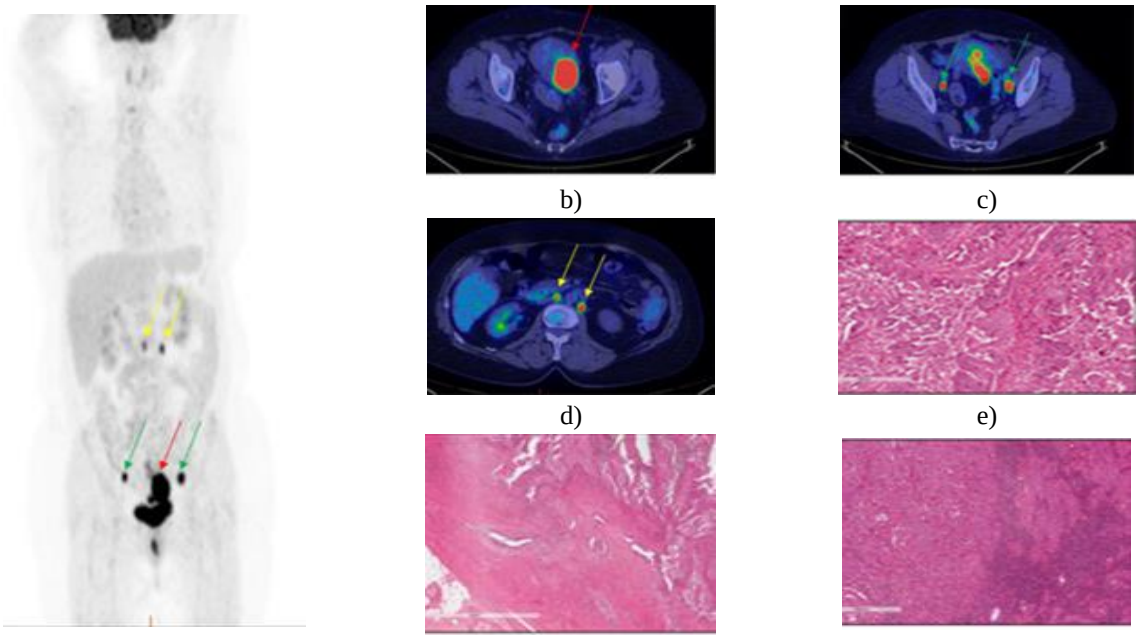

Figure 3. 18F-FDG PET/CT imaging used for staging endometrial carcinoma (EC).

A 71-year-old woman diagnosed with endometrial cancer (Stage III C1; Grade 3; non-endometrioid histotype; 85% myometrial invasion; high–intermediate/high risk group; with lymph node involvement) underwent 18F-FDG PET/CT for disease staging. Red arrows highlight abnormal FDG uptake at the primary tumor site, green arrows mark pathological uptake in bilateral iliac–obturator lymph nodes, and yellow arrows point to pathological uptake in lomboaortic and interaortocaval lymph nodes ((a): MIP image; (b–d): axial PET/CT slices). PET metrics of the primary lesion were as follows: SUVmax = 17.43; SUVmean = 11.82; MTV = 28.60; TLG = 338.04. Histopathology revealed a neoplasm composed of large cells showing marked nuclear atypia and abundant mitotic activity (e). The growth pattern was predominantly papillary. Myometrial invasion (f) displayed a tubulo-glandular pattern with micro-papillary structures within the lumen and an infiltrative/destructive invasion front. Lymph node metastasis (g) appeared as nodular deposits of serous atypical cells arranged in cords and small clusters.

Performance metrics including accuracy, sensitivity, specificity, negative predictive value (NPV), and positive predictive value (PPV) obtained by applying the derived cut-offs to the validation cohort are presented in **Table 4**. Notably, TLG yielded the highest accuracies for predicting deep myometrial invasion (61%) and lymph node involvement (72%), whereas SUVmax achieved the best accuracy (71%) for EC risk group stratification. Prediction of p53 expression status, however, remained limited (accuracy = 45%).

Table 4. Predictive performance of individual 18F-FDG PET parameters and clinical features alone or combined in random forest classifiers for predicting aggressive features of endometrial cancer in the validation set.

Aggressive feature of EC	Parameter	SUVmean	SUVmax	TLG	MTV	Age	Random forest classifier
Myometrial invasion	Optimal threshold	8.56	14.85	96.13	10.98	66.45	RFC_MI
	Accuracy	52%	52%	61%	52%	48%	87%
	Sensitivity	67%	67%	58%	42%	42%	100%
	Specificity	36%	36%	64%	64%	55%	73%
	Positive predictive value (PPV)	53%	53%	64%	56%	50%	80%
	Negative predictive value (NPV)	50%	50%	58%	50%	46%	100%
EC risk group	Optimal threshold	9.69	14.19	96.13	5.13	—	RFC_RG
	Accuracy	67%	71%	62%	54%	—	79%
	Sensitivity	50%	75%	58%	67%	—	92%
	Specificity	83%	67%	67%	42%	—	67%
	Positive predictive value (PPV)	75%	69%	64%	53%	—	73%
	Negative predictive value (NPV)	62%	73%	62%	56%	—	89%
Lymph node involvement	Optimal threshold	—	—	251.82	10.98	—	RFC_LN
	Accuracy	—	—	72%	61%	—	83%
	Sensitivity	—	—	25%	50%	—	25%
	Specificity	—	—	86%	64%	—	100%
	Positive predictive value (PPV)	—	—	33%	29%	—	100%
	Negative predictive value (NPV)	—	—	80%	82%	—	82%
p53 expression	Optimal threshold	9.54	16.29	—	—	—	RFC_p53
	Accuracy	45%	45%	—	—	—	73%
	Sensitivity	40%	20%	—	—	—	100%
	Specificity	50%	67%	—	—	—	50%
	Positive predictive value (PPV)	40%	33%	—	—	—	63%
	Negative predictive value (NPV)	50%	50%	—	—	—	100%

Optimal cut-off values for each PET parameter were determined from ROC curves in the training set and subsequently applied as thresholds (th) for patient classification in the validation set. Abbreviations: RFC = Random Forest Classifier; MI = myometrial invasion; RG = risk group; LN = lymph node.

Machine learning

For every indicator of EC aggressiveness, a random forest classifier (RFC) model was developed on the training dataset, specifically RFCMI, RFCRG, RFCLN, and RFCp53.

Input features for each model were selected based on AUC results on the training set **(Table 3)**, including only those parameters with 95% confidence intervals that were statistically significant. In detail, SUVmax, SUVmean, MTV, TLG, and age served as inputs for RFCMI; SUVmax, SUVmean, MTV, and TLG were used for RFCRG; MTV and TLG were used for RFCLN; and SUVmax and SUVmean were used for RFCp53. Bootstrap sampling was applied in all models, utilizing random subsets of the training data to construct the individual decision trees. To address class imbalance issues in forecasting EC risk group and lymph node involvement, the "class weight" setting was adjusted to give greater importance to the underrepresented class. Optimal hyperparameters were determined for each classifier and are outlined in **Table 5**.

Table 5. Hyperparameters selected for the implementation of the four random forest classifier (RFC) algorithms.

Hyperparameters	EC risk group	Myometrial invasion	Lymph node involvement	p53 expression
n_estimators	22	24	2	5
max_depth	None	None	None	None
min_samples_split	2	5	2	2

min_samples_leaf	4	2	1	1
max_features	auto	auto	auto	Auto
bootstrap	True	True	True	True
class_weight	1:2	1:1	1:1.5	1:1

Hyperparameters are defined according to the Scikit–learn library [39].

Predictions generated by the models on the validation cohort, including accuracy, sensitivity, specificity, NPV, and PPV, are summarized in **Table 4**. Specifically, deep myometrial invasion (MI) was correctly classified with 87% accuracy when incorporating all PET parameters plus age. EC risk group was predicted with 79% accuracy using all PET parameters. Lymph node (LN) involvement reached 83% accuracy utilizing MTV and TLG. Lastly, p53 expression was predicted with 73% accuracy using SUVmax and SUVmean.

This investigation highlights the clinical usefulness of machine learning-driven classification models built from standard 18F-FDG PET metrics and basic clinical information for forecasting key aspects of tumor aggressiveness in patients with endometrial carcinoma (EC) undergoing staging evaluation.

Our findings indicate that SUVmax and SUVmean effectively distinguish and predict deep MI, EC risk category, and p53 expression. Furthermore, the volumetric metabolic indices MTV and TLG demonstrated strong performance in anticipating deep MI, EC risk group, and LN involvement. In contrast, no imaging parameter demonstrated the capacity to discriminate or predict histological subtype. The performance of these PET variables was further benchmarked against routine clinical factors previously linked to EC risk, such as patient age and BMI. Both proved to have minimal predictive value, with age alone showing some association with deep MI.

The outcomes align with several earlier reports in the literature. Prior studies noted significantly elevated SUVmax in the primary tumor among high-risk EC patients relative to low-risk cases, reporting sensitivities and specificities of 74% and 46% for risk group differentiation (compared with 75% and 61% in the current analysis) [44]. Comparable agreements were observed with previous research exploring links between SUV parameters and deep myometrial invasion [45, 46]. Regarding metabolic volume indices, certain authors have proposed MTV and TLG as potential indicators of LN involvement [47]; the present results support this view, identifying MTV and TLG as the sole parameters capable of both discriminating and predicting nodal metastases. Notably, the observation that 18F-FDG PET can help predict p53 overexpression represents a novel contribution, particularly relevant given p53's established prognostic importance in EC [48]. Molecular profiling of EC is now incorporated into standard clinical practice for risk stratification, as endorsed by ESGO/ESTRO/ESP guidelines, thereby improving accuracy beyond traditional clinicopathological factors such as histological subtype, grade, and depth of invasion [25].

A key advantage of this study over much of the existing literature is the inclusion of an independent validation cohort, enabling evaluation of the selected cut-offs and model performance on unseen data. Such validation remains relatively rare in conventional statistical analyses of PET in EC. This design offered a more robust preliminary assessment of the real-world utility of the investigated parameters for patient stratification, yielding direct measures of accuracy, sensitivity, specificity, NPV, and PPV. It also permitted evaluation of whether machine learning approaches could provide added benefit in this context. ML applications in molecular imaging for EC remain scarce, with most existing work focused on MRI datasets [49-52] and only limited reports using 18F-FDG PET [53]. Importantly, those studies primarily relied on radiomic features. To our knowledge, the current study is the first to examine conventional semiquantitative PET parameters (potentially combined with clinical variables) through ML models for primary staging of EC. This approach enhances clinical interpretability and facilitates practical implementation, since the parameters can be readily obtained on standard imaging workstations and software.

Nevertheless, several limitations must be acknowledged. Although 123 patients were enrolled, complete histological confirmation of all aggressiveness features was not available for every case, requiring the creation of smaller subgroups with appropriate reference standards. Class imbalance was also evident, particularly in the assessment of LN involvement. To the best of our knowledge, no prior research has evaluated 18F-FDG PET-based ML using conventional parameters from the primary tumor to predict deep MI, EC risk group, LN

status, and p53 expression. Consequently, larger and more balanced cohorts are warranted to validate these findings. Additionally, the study was conducted at a single center, so external validation using independent datasets from other institutions will be essential to confirm model generalizability and robustness.

Conclusion

This study presents one of the earliest evaluations of machine learning classification based on 18F-FDG PET-derived parameters for preoperative prediction of EC aggressiveness features, which are otherwise only determined postoperatively despite their importance for optimal treatment planning. A predictive signature combining standard PET metrics (SUVmax, SUVmean, TLG, and MTV) with clinical variables (age and BMI) was developed to provide clinicians with an interpretable and easily translatable tool. The results demonstrate that this strategy can effectively characterize several critical aspects of EC aggressiveness preoperatively, including histological subtype, presence of deep myometrial invasion (MI), lymph node involvement (LN), p53 expression status (wild-type versus mutated), and overall risk group. These findings underscore the potential of advanced yet accessible PET image analysis—leveraging conventional quantitative parameters and machine learning—to improve non-invasive preoperative risk stratification and guide management decisions in patients with EC.

Acknowledgments: None

Conflict of Interest: None

Financial Support: None

Ethics Statement: None

References

1. Koskas M, Amant F, Mirza MR, Creutzberg CL. Cancer of the corpus uteri: 2021 update. Int J Gynecol Obstet. 2021;155:45–60.
2. Poole EM, Lin WT, Kvaskoff M, De Vivo I, Terry KL, Missmer SA. Endometriosis and risk of ovarian and endometrial cancers in a large prospective cohort of U.S. nurses. Cancer Causes Control. 2017;28:437–45.
3. Ali AT. Risk factors for endometrial cancer. Ceska Gynekol. 2013;78:448–59.
4. Ferlay J, Shin HR, Bray F, Forman D, Mathers C, Parkin DM. Estimates of worldwide burden of cancer in 2008: GLOBOCAN 2008. Int J Cancer. 2010;127:2893–917.
5. Morice P, Leary A, Creutzberg C, Abu-Rustum N, Darai E. Endometrial cancer. Lancet. 2016;387:1094–108.
6. Makker V, Taylor MH, Aghajanian C, Oaknin A, Mier J, Cohn AL, et al. Lenvatinib Plus Pembrolizumab in Patients with Advanced Endometrial Cancer. J Clin Oncol. 2020;38:2981–92.
7. Noriega-Álvarez E, García Vicente AM, Jiménez Londoño GA, Martínez Bravo WR, González García B, Soriano Castrejón ÁM. A systematic review about the role of preoperative 18F–FDG PET/CT for prognosis and risk stratification in patients with endometrial cancer. Rev Esp Med Nucl Imagen Mol (Engl Ed). 2021; in press.
8. Giampaolino P, Cafasso V, Boccia D, Ascione M, Mercorio A, Viciglione F, et al. Fertility–Sparing Approach in Patients with Endometrioid Endometrial Cancer Grade 2 Stage IA (FIGO): A Qualitative Systematic Review. Biomed Res Int. 2022;2022:4070368.
9. Mutlu L, Manavella DD, Gullo G, McNamara B, Santin AD, Patrizio P. Endometrial Cancer in Reproductive Age: Fertility–Sparing Approach and Reproductive Outcomes. Cancers. 2022;14:5187.
10. Zaami S, Stark M, Signore F, Gullo G, Marinelli E. Fertility preservation in female cancer sufferers: (only) a moral obligation? Eur J Contracept Reprod Health Care. 2022;27:335–40.
11. Berman ML, Ballon SC, Lagasse LD, Watring WG. Prognosis and treatment of endometrial cancer. Am J Obstet Gynecol. 1980;136:679–88.
12. Larson D, Connor G, Broste S, Krawisz B, Johnson K. Prognostic significance of gross myometrial invasion with endometrial cancer. Obstet Gynecol. 1996;88:394–8.
13. Boronow RC, Morrow CP, Creasman WT, Disaia PJ, Silverberg SG, Miller A, et al. Surgical staging in endometrial cancer: Clinical–pathologic findings of a prospective study. Obstet Gynecol. 1984;63:825–32.
14. Rizzo S, Femia M, Buscarino V, Franchi D, Garbi A, Zanagnolo V, et al. Endometrial cancer: An

overview of novelties in treatment and related imaging keypoints for local staging. Cancer Imaging. 2018;18:45.
15. Tanos P, Dimitriou S, Gullo G, Tanos V. Biomolecular and Genetic Prognostic Factors That Can Facilitate Fertility–Sparing Treatment (FST) Decision Making in Early Stage Endometrial Cancer (ES–EC): A Systematic Review. Int J Mol Sci. 2022;23:2653.
16. Eritja N, Navaridas R, Ruiz-Mitjana A, Vidal-Sabanés M, Egea J, Encinas M, et al. Endometrial PTEN Deficiency Leads to SMAD2/3 Nuclear Translocation. Cancers. 2021;13:4990.
17. Yang H, Han F, Hu R, Liu J, Sui J, Xiang X, et al. PTEN gene mutations correlate to poor prognosis in glioma patients: A meta-analysis. OncoTargets Ther. 2016;2016:3485.
18. Boussios S, Rassy E, Shah S, Ioannidou E, Sheriff M, Pavlidis N. Aberrations of DNA repair pathways in prostate cancer: A cornerstone of precision oncology. Expert Opin Ther Targets. 2021;25:329–33.
19. Daix M, Aida Angeles M, Migliorelli F, Kakkos A, Martinez Gomez C, Delbecque K, et al. Concordance between preoperative ESMO–ESGO–ESTRO risk classification and final histology in early–stage endometrial cancer. J Gynecol Oncol. 2021;32:e48.
20. Helpman L, Kupets R, Covens A, Saad RS, Khalifa MA, Ismiil N, et al. Assessment of endometrial sampling as a predictor of final surgical pathology in endometrial cancer. Br J Cancer. 2014;110:609–15.
21. Dou Y, Kawaler EA, Cui Zhou D, Gritsenko MA, Huang C, Blumenberg L, et al. Proteogenomic Characterization of Endometrial Carcinoma. Cell. 2020;180:729–48.e26.
22. Bezzi C, Zambella E, Ghezzo S, Fallanca F, Samanes Gajate AM, Franchini A, et al. 18F–FDG PET/MRI in endometrial cancer: Systematic review and meta-analysis. Clin Transl Imaging. 2021;10:45–58.
23. Capozzi VA, Rosati A, Rumolo V, Ferrari F, Gullo G, Karaman E, et al. Novelties of ultrasound imaging for endometrial cancer preoperative workup. Minerva Med. 2021;112:3–11.
24. Colombo N, Creutzberg C, Amant F, Bosse T, González-Martón A, Ledermann J, et al. ESMO–ESGO–ESTRO consensus conference on endometrial cancer: Diagnosis, treatment and follow-up. Ann Oncol. 2016;27:16–41.
25. Concin N, Matias-Guiu X, Vergote I, Cibula D, Mirza MR, Marnitz S, et al. ESGO/ESTRO/ESP guidelines for the management of patients with endometrial carcinoma. Int J Gynecol Cancer. 2021;31:12–39.
26. Faria SC, Devine CE, Rao B, Sagebiel T, Bhosale P. Imaging and Staging of Endometrial Cancer. Semin Ultrasound CT MRI. 2019;40:287–94.
27. Picchio M, Mangili G, Samanes Gajate AM, De Marzi P, Spinapolice EG, Mapelli P, et al. High–grade endometrial cancer: Value of [18F]FDG PET/CT in preoperative staging. Nucl Med Commun. 2010;31:506–12.
28. Gee MS, Atri M, Bandos AI, Mannel RS, Gold MA, Lee SI. Identification of distant metastatic disease in uterine cervical and endometrial cancers with FDG PET/CT: Analysis from the ACRIN 6671/GOG 0233 Multicenter Trial. Radiology. 2018;287:176–84.
29. Mapelli P, Ironi G, Bergamini A, Mangili G, Paola R, Taccagni GL, et al. Synergic role of preoperative 18F–fluorodeoxyglucose PET and MRI parameters in predicting histopathological features of endometrial cancer. Nucl Med Commun. 2020;41:1073–80.
30. Ironi G, Mapelli P, Bergamini A, Fallanca F, Candotti G, Gnasso C, et al. Hybrid PET/MRI in Staging Endometrial Cancer. Clin Nucl Med. 2022;47:221–9.
31. Sollini M, Bandera F, Kirienko M. Quantitative imaging biomarkers in nuclear medicine: From SUV to image mining studies. Highlights from annals of nuclear medicine 2018. Eur J Nucl Med Mol Imaging. 2019;46:2737–45.
32. Gillies RJ, Kinahan PE, Hricak H. Radiomics: Images are more than pictures, they are data. Radiology. 2016;278:563–77.
33. Mapelli P, Partelli S, Salgarello M, Doraku J, Muffatti F, Schiavo Lena M, et al. Dual tracer 68Ga-DOTATOC and 18f–FDG PET improve preoperative evaluation of aggressiveness in resectable pancreatic neuroendocrine neoplasms. Diagnostics. 2021;11:192.
34. Christensen TN, Andersen PK, Langer SW, Fischer BMB. Prognostic Value of 18F–FDG–PET Parameters in Patients with Small Cell Lung Cancer:

A Meta–Analysis and Review of Current Literature. Diagnostics. 2021;11:174.
35. Wang H, Dai H, Li Q, Shen G, Shi L, Tian R. Investigating 18F–FDG PET/CT Parameters as Prognostic Markers for Differentiated Thyroid Cancer: A Systematic Review. Front Oncol. 2021;11:648658.
36. Bezzi C, Monaco L, Ghezzo S, Mathoux G, Bergamini A, Zambella E, et al. 18F–FDG PET/CT May Predict Tumor Type and Risk Score in Gestational Trophoblastic Disease. Clin Nucl Med. 2022;47:525–31.
37. Ngiam KY, Khor IW. Big data and machine learning algorithms for health–care delivery. Lancet Oncol. 2019;20:e262–73.
38. Orlhac F, Eertink JJ, Cottereau A-S, Zijlstra JM, Thieblemont C, Meignan M, et al. A Guide to ComBat Harmonization of Imaging Biomarkers in Multicenter Studies. J Nucl Med. 2022;63:172–9.
39. Pedregosa F, Varoquaux G, Gramfort A, Michel V, Thirion B, Grisel O, et al. Scikit–learn: Machine Learning in Python. J Mach Learn Res. 2011;12:2825–30.
40. Bettinardi V, Danna M, Savi A, Lecchi M, Castiglioni I, Gilardi MC, et al. Performance evaluation of the new whole–body PET/CT scanner: Discovery ST. Eur J Nucl Med Mol Imaging. 2004;31:867–81.
41. Tarantola G, Zito F, Gerundini P. PET instrumentation and reconstruction algorithms in whole–body applications. J Nucl Med. 2003;44:756–69.
42. Sathiakumar C, Som S, Eberl S, Lin P. NEMA NU 2-2001 performance testing of a Philips Gemini GXL PET/CT scanner. Australas Phys Eng Sci Med. 2010;33:199–209.
43. Bettinardi V, Presotto L, Rapisarda E, Picchio M, Gianolli L, Gilardi MC. Physical Performance of the new hybrid PETCT Discovery–690. Med Phys. 2011;38:5394–411.
44. Ghooshkhanei H, Treglia G, Sabouri G, Davoodi R, Sadeghi R. Risk stratification and prognosis determination using 18F–FDG PET imaging in endometrial cancer patients: A systematic review and meta-analysis. Gynecol Oncol. 2014;132:669–76.
45. Torizuka T, Nakamura F, Takekuma M, Kanno T, Ogusu T, Yoshikawa E, et al. FDG PET for the assessment of myometrial infiltration in clinical stage I uterine corpus cancer. Nucl Med Commun. 2006;27:481–7.
46. Walentowicz-Sadłecka M, Sadłecki P, Małecki B, Walentowicz P, Marszałek A, Domaracki P, et al. SUVmax measured by 18F FDG PET/CT in the primary tumor in relation to clinical and pathological features of endometrial cancer. Pol Gynaecol. 2013;84:748–53.
47. Crivellaro C, Signorelli M, Guerra L, De Ponti E, Pirovano C, Fruscio R, et al. Tailoring systematic lymphadenectomy in high–risk clinical early stage endometrial cancer: The role of 18F–FDG PET/CT. Gynecol Oncol. 2013;130:306–11.
48. Perrone E, De Felice F, Capasso I, Distefano E, Lorusso D, Nero C, et al. The immunohistochemical molecular risk classification in endometrial cancer: A pragmatic and high–reproducibility method. Gynecol Oncol. 2022;165:585–93.
49. Stanzione A, Cuocolo R, Del Grosso R, Nardiello A, Romeo V, Travaglino A, et al. Deep Myometrial Infiltration of Endometrial Cancer on MRI: A Radiomics–Powered Machine Learning Pilot Study. Acad Radiol. 2021;28:737–44.
50. Otani S, Himoto Y, Nishio M, Fujimoto K, Moribata Y, Yakami M, et al. Radiomic machine learning for pretreatment assessment of prognostic risk factors for endometrial cancer and its effects on radiologists' decisions of deep myometrial invasion. Magn Reson Imaging. 2022;85:161–7.
51. Rodríguez-Ortega A, Alegre A, Lago V, Carot-Sierra JM, Ten-Esteve A, Montoliu G, et al. Machine Learning–Based Integration of Prognostic Magnetic Resonance Imaging Biomarkers for Myometrial Invasion Stratification in Endometrial Cancer. J Magn Reson Imaging. 2021;54:987–95.
52. Yang LY, Siow TY, Lin YC, Wu RC, Lu HY, Chiang HJ, et al. Computer–aided segmentation and machine learning of integrated clinical and diffusion–weighted imaging parameters for predicting lymph node metastasis in endometrial cancer. Cancers. 2021;13:1406.
53. Nakajo M, Jinguji M, Tani A, Kikuno H, Hirahara D, Togami S, et al. Application of a Machine Learning Approach for the Analysis of Clinical and Radiomic Features of Pretreatment [18F]–FDG PET/CT to Predict Prognosis of Patients with Endometrial Cancer. Mol Imaging Biol. 2021;23:756–65.